JCTC Journal of Chemical Theory and Computation

Binding of Gold Nanoclusters with Size-Expanded DNA Bases: A Computational Study of Structural and Electronic Properties

Purshotam Sharma, Himanshu Singh, Sitansh Sharma, and Harjinder Singh*

Center for Computational Natural Sciences and Bioinformatics, International Institute of Information and Technology, Gachibowli, Hyderabad-500032, India

Received June 15, 2007

Abstract: Binding of gold nanoclusters with size-expanded DNA bases, xA, xC, xG, and xT, is studied using quantum chemical methods. Geometries of the neutral xA-Au_6, xC-Au_6, xG-Au_6, and xT-Au_6 complexes were fully optimized using the B3LYP density functional method (DFT). The gold clusters around xA and xT adopt triangular geometries, whereas irregular structures are obtained in the case of gold clusters complexed around xC and xG. The lengths of the bonds between atoms in the x-bases increase on gold complexation. The aromatic character of the x-bases also increases on gold complexation except for the five-member rings. A significant charge transfer from the x-base to gold atoms is seen in these complexes. Second-order interactions are observed in addition to direct covalent bonds between gold atoms and x-bases.

1. Introduction

Detailed understanding of the nature of interaction between metal particles and conjugated molecular systems in nanoparticle complexes is of fundamental importance in the development of potential miniature devices.[1a,b] Interest in the use of modified analogs of DNA as templates for growing nanoparticle complexes has increased significantly in recent years simultaneous with intensive investigations on whether alternative genetic systems could exist for therapeutic and biotechnological applications. Analogs such as peptide nucleic acids (PNAs),[2a,b] locked nucleic acids (LNAs),[3a] and threose nucleic acids (TNAs)[3b,c] have been synthesized by different research groups. In most cases, mainly the backbone of DNA has been subject to chemical modifications. Kool and co-workers have synthesized new modified DNA using size-expanded DNA bases called xDNA[4] and yDNA.[5] It is believed that size-expanded DNA could also have properties with potential nanotechnological applications, as they retain the recognition property of natural DNA to a certain extent. These size-expanded bases are formed by benzohomologation of the natural DNA bases. They pair with complementary normal DNA bases in size-expanded DNA. More recently xDNA Double Helix up to eight base pairs incorporating all four combinations of the x-bases and natural DNA bases has been prepared.[6]

The controlled assembly of metal nanoparticles into macroscopic materials using DNA oligonucleotides has opened new directions of research in nanosciences. The charge transport properties of DNA are of great importance in the development of nanotechnological devices.[7,8] It is known that metal bound DNA nanowires have enhanced conductivity.[8,9] A large number of experimental and theoretical studies are focused on gold-DNA interactions.[10a−j] Gold, known as a noble metal for its relatively inert chemistry, has turned out to be of remarkable use in a large number of investigations of nanobio systems. Molecular dynamics simulations have been carried out in order to understand the melting properties of DNA-linked gold nanoparticle assemblies.[10g] Ab initio calculations have been carried out on bare and thiolate passivated gold nanoclusters, gold nanowires, and fragments of DNA chains, in order to provide useful insights toward the complete understanding, design, and proper utilization of hybrid DNA-gold nanostructured materials.[10h] Theoretical studies on gold nanoparticles conjugated with small organic compounds such as acetone, acetaldehyde, and diethyl ketone have also been carried out recently.[10i]

* Corresponding author phone: +91 40 2300 1967 x277; fax: +91 40 2300 1413; e-mail: laltu@iiit.ac.in.

10.1021/ct700145e CCC: $37.00
Published on Web 10/16/2007

A few theoretical studies have been carried out regarding the structural and electronic properties of the x-bases.[11] The extra Π-electrons on benzene ring in the size-expanded DNAs induce stronger Π-Π coupling between stacked bases, that would facilitate band transport. It is established that metal bound natural DNA can be a good nanowire. Experimental and theoretical studies on the nature of binding between gold nanoclusters and natural DNA bases and base pairs have been reported.[12−14] Experiments showed that adenine (A), cytosine (C), guanine (G), and thymine (T) nucleobases interact specifically and in a sequence dependent manner with the Au surfaces.[12]

Using density functional theory techniques, we explore in this work the nature of binding between gold clusters and size-expanded bases and try to understand what similarities exist and what differences would arise in these structures as compared to natural bases. We are mainly interested in investigating the structural and electronic properties of metal bound size-expanded DNA bases and the nature of interaction between xDNA bases and metal atoms. The optimized structures of gold atoms bound to x-bases show features similar to earlier works on DNA bases.[15] Irregular structures as well as Au−Au distances seen by us are similar to those obtained in the study of a thiolate molecule anchored on a stepped gold surface leading to the formation of a monatomic gold nanowire, by Krüger et al.[15] The results from these analysis may lead to the possibility of newer families of nanowires and other technologically relevant devices.

2. Methods

The Gaussian03[16] suite of programs was used for all calculations. The initial geometries of individual bases were built from the coordinates extracted from NMR models of size-expanded DNA from Protein Data Bank (PDB) for xDNA (code: 2ICZ). After removal of phosphate and sugar backbones, the structures of xA, xC, xG, and xT were optimized using the HF-6-31G** basis set. The initial structures for the gold complexes were built by placing x-bases within two equilateral gold triangles using the HF-6-31G** optimized geometries of the x-bases as the initial starting point. These structures were optimized using B3LYP/LANL2MB basis sets. Vibrational analysis was carried out for all optimized structures, and real frequencies were obtained in all cases. Single point energy calculations followed by vibrational analysis were also carried out at the B3LYP/LANL2MB level on the HF-6-31G** optimized geometries of free x-bases, in order to allow meaningful comparisons of different characteristics of x-base structures before and after gold complexation at the same theoretical level.

A measure of changes in the chemical environment of atoms in aromatic molecules is the nucleus independent chemical shift[17] in NMR measurements. We have calculated these shifts for the free x-bases and those coupled to gold clusters. The nucleus independent chemical shifts (NICS) method allows the evaluation of aromaticity, antiaromaticity, and nonaromaticity of single ring systems and individual rings in polycyclic systems (local aromaticities). This method has been extensively used to assess the aromaticity and antiaromaticity of many organic and inorganic compounds, intermediates, and transition states.[18] Recently, total NICS values were used to assess the aromaticities of different polycyclic aromatic hydrocarbons with excellent agreement with other indices of aromaticity. A ghost atom placed in the center of the five- and six-member rings of these x-bases provides a measure of the shielding effect of ring current, which gives a measure of NICS.

Additionally, Natural Bond Orbital (NBO)[19] analysis was performed on the B3LYP/LanL2MB optimized structures, to find the second-order interactions among electrons in these molecular clusters.

3. Results

We describe below the results obtained followed by a discussion in the next section. Only select data are recorded in this article. Tables (labeled Sn) of data with complete details are given in the Supporting Information. The structures of optimized xDNA bases together with corresponding natural DNA bases (insets) are shown in Figure 1. It is known from earlier studies on natural DNA bases that the gold atoms act predominantly as acceptors of electronic charge from the DNA system.[12] The starting geometries of molecular clusters consisting of the x-bases and gold atoms for optimization were generated by placing two clusters consisting of three gold atoms each, near the atoms with relatively high electronegativity, O and N, of the x-bases in their optimized geometry (we use the generic term x-bases to indicate the size-expanded bases). The optimized structures of neutral x-DNA bases complexed with six gold atoms are shown in Figure 2 (coordinates in Table S1). The nonplanarity in the (xBase)-Au_6 complexes is measured in terms of relevant dihedral angles (Table 1a).

It is seen generally that on interacting with the gold atoms, all bonds tend to expand, and the electronic charges on atoms in the bases tend to decrease. The magnitudes of a few selected bond lengths in x-bases before and after complex formation with gold atoms are given in Table 1b and the same with several others in Table S2 in the Supporting Information. The changes in bond lengths on formation of complexes with the gold atoms have been compared for some selected common bonds in natural purines and x-purines in Figure 3(a) and in natural pyrimidines and x-pyrimidines in Figure 3(b), respectively. Mulliken population analysis was looked into. Extensive comparative histograms are plotted in Figure 4 to show the Mulliken charges over all the atoms in the bases before and after complexation, and the detailed data are given in Table S3.

The shapes and orientation of frontier molecular orbitals are a good indication of reactivity of chemical systems. Plots of highest occupied molecular orbital (HOMO) and lowest unoccupied molecular orbital (LUMO) for the x-bases are given in Figure 5. The plots of HOMO, HOMO-1, and LUMO for gold complexed x-bases are given in Figure 6.

The changes in vibrational frequencies on complexation with gold for some selected bonds of the x-bases have been given in Table 2. We see a red shift in the stretching frequencies of amino and carbonyl groups indicating weakening of these bonds in synchrony with the increase of corresponding bond lengths.

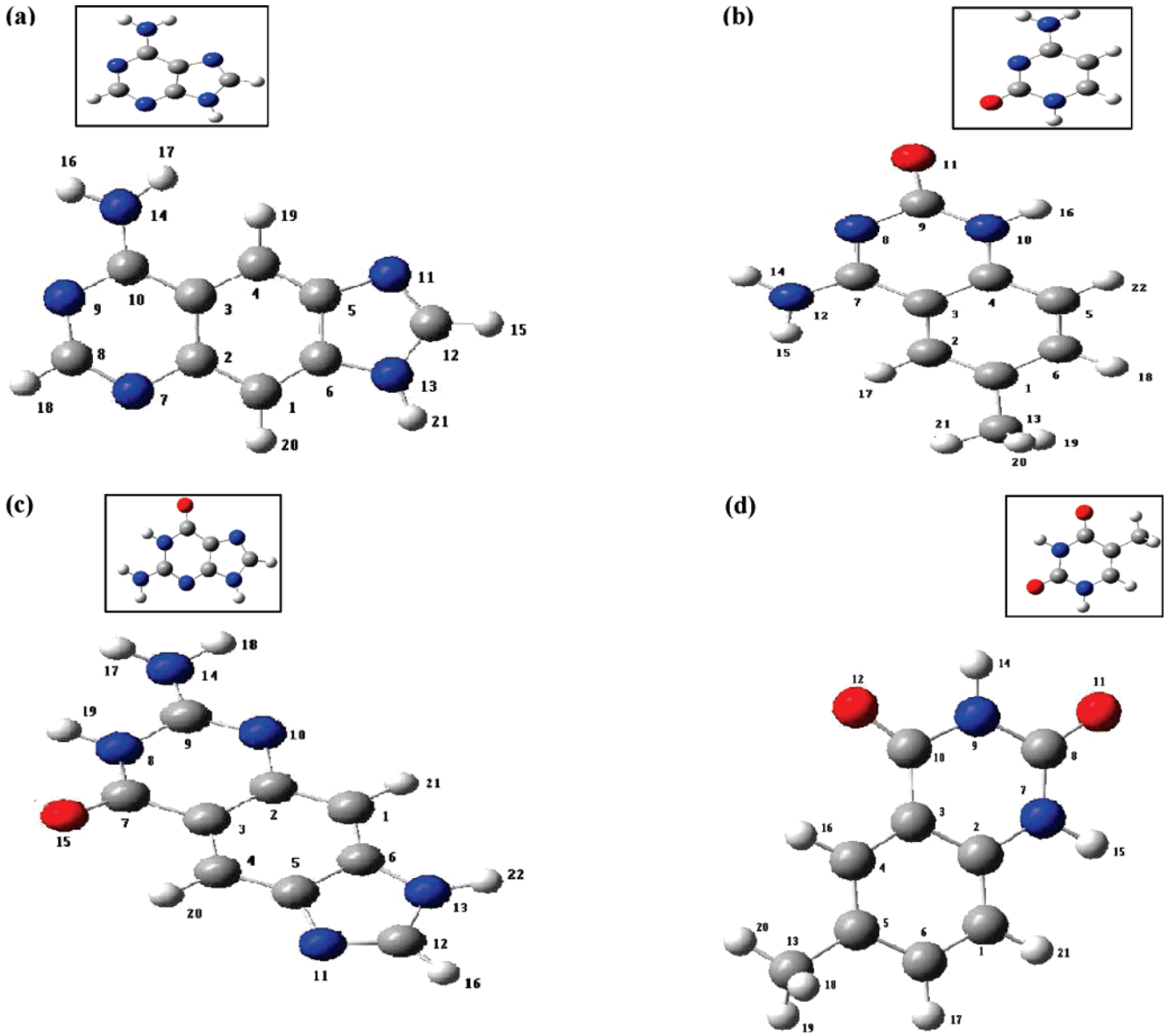

Figure 1. Size-expanded DNA bases (x-bases): (a) xA, (b) xC, (c) xG, and (d) xT. Insets show corresponding natural DNA bases. Color code: oxygen, red; carbon, dark gray; nitrogen, blue; and hydrogen, light gray.

The nucleus independent chemical shifts (NICS) for the aromatic rings of the x-bases before and after gold complexation are given in Table 3. It is found that there is a general increase in the NICS values on complexation. This is an indication of increase in the aromatic character after complex formation. In order to better understand the nature of binding between gold atoms and atoms of the x-bases, the second-order interactions present between electron density on gold atoms and on atoms of the x-bases were calculated using second-order perturbation theory analysis of gold complexed x-bases. A select cross-section of the NBO data is given in Table 4, and more detailed information is available in Table S4. The NBO analysis predicts certain second-order noncovalent interactions, in addition to direct covalent bonding between x-bases and gold clusters.

4. Discussion

Structures of Complexes. As mentioned earlier, we started the geometry optimization with placing three gold atoms near the relatively more electronegative elements, O and N, on two sides of the bases. The initial geometries of these complexes were built by placing two gold clusters, each of them forming an equilateral triangle on each side of the x-adenine near the electron rich sites, in order to model the first layer of the 111 face-centered cubic (FCC) bulk gold crystal. No change in the optimized structures was seen on using other structures in a wide neighborhood. We will generally refer to the complexes as xB-Au_6 complex except when it is imperative to indicate that they form two separate Au_3 clusters. It is found that structures obtained on optimization of x-adenine-Au_6 and x-cytosine-Au_6 complexes are nearly planar, with both the Au_6 cluster as well as the x-base separately adopting planar geometries. On the other hand, the optimized structures of x-guanine-Au_6 and x-thymine-Au_6 are significantly nonplanar. This absence of planarity in the xG-Au_6 and xT-Au_6 (the respective x-bases are planar in both cases) is noteworthy. It is possibly due to the anisotropy in electronic distribution around the x-DNA base.

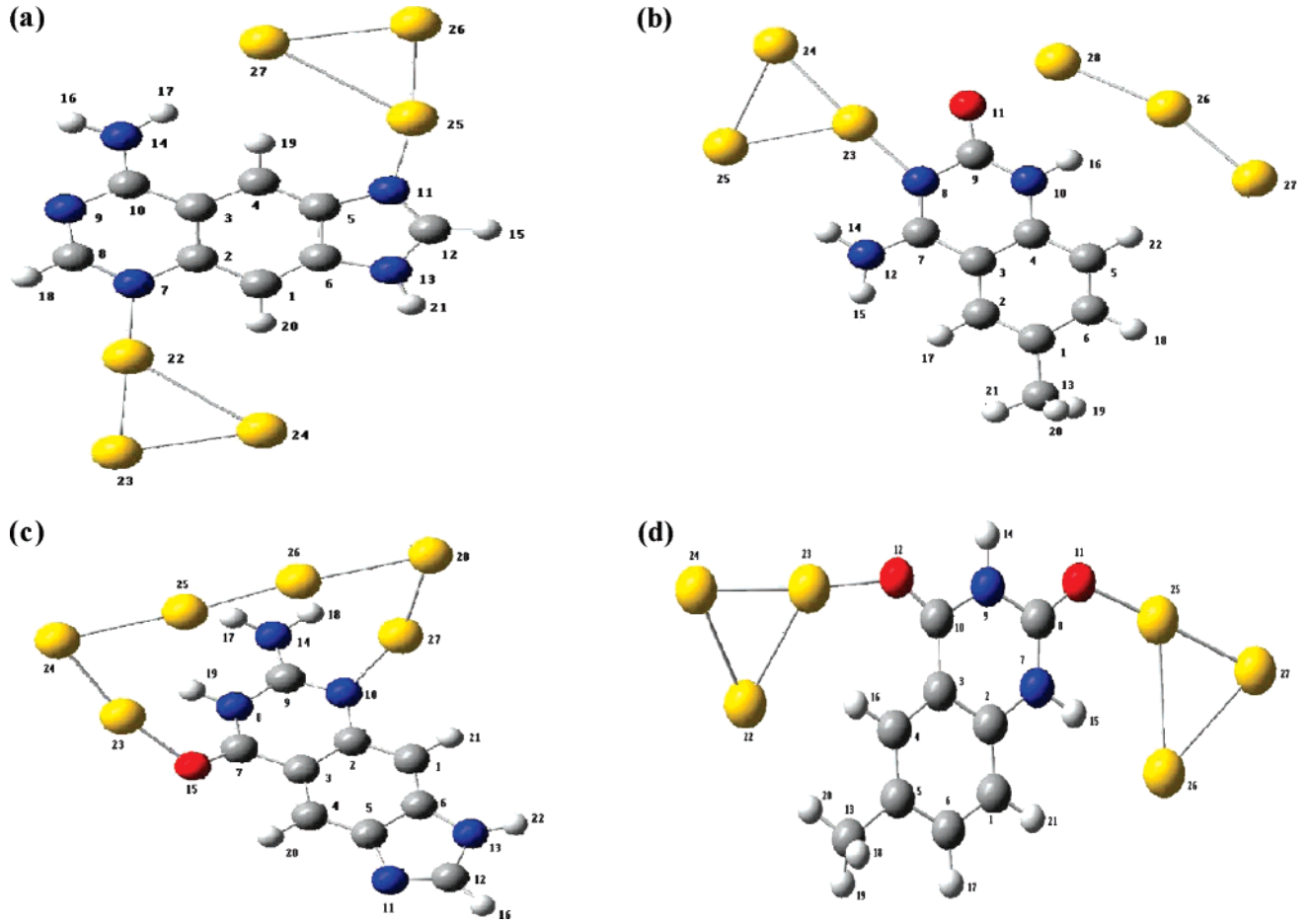

Figure 2. Optimized structures of (a) xA-Au_6 (b) xC-Au_6 (c) xG-Au_6, and (d) xT-Au_6, obtained at the B3LYP/LanL2MB level of theory.

In xG-Au_6, four of the six gold atoms are relatively closer to the base thus disrupting the consistency of the Au_3 cluster which remains preserved in the case of xA-Au_6 and xC-Au_6 complexes. In this sense, the general use of the word 'cluster' for the Au_3 units may be debatable.

A general trend seen is that the gold atoms bind to electron rich sites of the x-bases (N or O atoms). When bare nitrogen atoms (having no hydrogens attached) are available, at least one of the gold atoms (in some cases two) in the (x-base)-Au_6 complexes preferably bind to the bare nitrogen atoms forming anchor bonds, whereas the gold atoms which are near to the N−H nitrogens form unconventional N−H...Au type of hydrogen bonds. In these cases, the gold atoms optimize to geometries with minimal Au−N distances. In the case of x-thymine, where the bare nitrogen atoms are absent, the gold atoms bind to oxygen atoms.

In xA-Au_6, the gold atoms are distributed in two clusters of three atoms each, near the nitrogen atoms of xA. Although both the Au_3 clusters acquire a triangular geometry, the edges of these triangles are not equal in length. The N11−Au25 and N7−Au22 bond lengths (Table 1b) are comparable to the Au−N distance in coordination complexes of gold and nitrogen containing ligands[20] suggesting a substantial Au−N covalent binding. In xC-Au_6, two clusters of three gold atoms each are distributed near the heterocyclic ring of the xC base, where the electron rich N and O atoms are present. One of these is present near the N8 atom and is triangular in geometry. The other cluster is present near the N10 and O11 atoms and is almost linear in geometry (Table 1a). The closest interaction between the gold atoms and the ring atoms of the xC is between the N8 and Au23 for the triangular cluster and between O11 and Au28 for the other cluster (Table 1b). The gold atoms in the xG-Au_6 complex also acquire an irregular geometry, forming a Au_6 unit, in contrast to the other complexes. The gold atoms are distributed near the six-member heterocyclic ring of the xG base, and the cluster geometry deviates slightly from planarity (Table 1). The closest interaction of gold cluster and base is between O15−Au23 (2.17 Å) atoms (Table 1b). In xT-Au_6, the gold atoms arrange themselves in the form of two triangles on each side of the base xT. These Au_3 triangles are not in the plane of the x-base; they are placed on different sides of the base. A triangular geometry of three gold atoms is present near the O12 atom of the base. The other Au_3 cluster is present near the O11 and O7 atoms of the xT. The O11−Au25 and the O12−Au23 constitute the closest interactions (Table 1b). In all these studied complexes the major interaction between gold atoms and x-bases is seen to arise from covalent binding of either Au−N or Au−O type.

A major structural change observed in all the x-bases that are anchored to Au_6 clusters is the overall increase in all the bond lengths of the x-bases, leading to an expansion in their volume. In most cases, the change is small, less than 0.1 Å,

Table 1. (a) Selected Dihedral Angles (deg) of Gold Complexed x-Bases and (b) Selected Bond Lengths before and after Complex Formation with Gold Atoms

(a)

x-adenine-Au_6		x-cytosine-Au_6	
∠C2−N7−Au 22−Au 23	178.80	∠Au 24−Au 23−O8−C7	179.05
∠C5−N11−Au 25−Au 26	0.05	∠Au 26−Au 28−O11−C9	0.03
∠Au 22−N7−C2−C3	179.99	∠Au 25−Au 23−Au 28−Au 26	179.75
∠Au 23−Au 22−Au 2−Au27	−179.89		
x-guanine-Au_6		**x-thymine-Au_6**	
∠Au 24−Au 23−N8−C9	39.07	∠Au 24−Au 23−O12−C10	−154.54
∠Au 25−Au 28−C9−N8	−19.62	∠Au 27−Au 25−O11−C8	5.23
∠Au 26−Au27−N10−C9	33.61	∠O12−C10−C8−O11	0.94
∠Au 24−Au 23−Au 25−Au 28	178.01	∠Au 26−N7−C8−N9	179.50
∠Au 25−Au 28−Au 27−Au 26	−177.13	∠Au 23−C3−C10−N9	−149.50

(b)

bond	xA	xA-Au_6	bond	xC	xC-Au_6	bond	xG	xG-Au_6	bond	xT	xT-Au_6
C12−N11	1.28	1.36	C7−N12	1.32	1.37	C9−N10	1.28	1.37	C2−N7	1.38	1.43
N11−C5	1.39	1.44	C7−N8	1.31	1.39	C2−N10	1.38	1.45	N17−H15	0.99	1.06
N7−C2	1.37	1.44	N8−C9	1.36	1.42	C7−O15	1.21	1.30	N7−C8	1.37	1.40
N7−C8	1.28	1.39	C9−O11	1.21	1.34	C7−N8	1.37	1.43	C8−O11	1.20	1.29
C10−N14	1.34	1.37	C9−N10	1.37	1.40	N8−C9	1.37	1.42	C8−N9	1.37	1.43
C10−N9	1.31	1.40	N10−H16	0.99	1.06	C9−N14	1.34	1.40	N9−C10	1.37	1.43
N9−C8	1.35	1.38	N10−C4	1.37	1.43	N14−H18	0.99	1.05	C10−O12	1.20	1.29
C8−H18	1.08	1.11	N12−H15	0.99	1.04	C12−N11	1.27	1.35	O12−Au23		2.12
N14−H16	1.00	1.04	N12−H14	1.01	1.05	C5−N11	1.39	1.45			
N7−Au22		2.10	O11−Au28		1.35	Au27−N10		2.16			
N11−Au25		2.11	N8−Au23		2.15	O18−Au23		2.17			

and, in a few cases, the increase is more than 0.1 Å. Such a pervasive increase, seen even in bonds located farthest from the Au atoms, reflects the electronic density redistribution caused by the gold clusters (discussed in detail later). In all the cases, the C−N and C−O bonds show a greater expansion than the C−C bonds. The interaction with gold atoms enhances the polarity of the bonds between atoms of different electronegativity in the base, causing a significant redistribution of charge and a consequent increase in bond lengths. The optimized geometries of these base-Au complexes suggest predominant interaction of the gold atoms with electron rich regions in the bases involving mainly the hetero atoms like N and O. These atoms make their nonbonding electrons available for interaction via molecular orbitals of suitable energy. The C═C bonds are parts of too low-lying MOs and are not suitable for interaction with the gold atoms. The HOMO, LUMO diagrams suggest that the HOMO electrons which are crucial in determining the reactivity of complexes with Au atom are mainly concentrated on the polar bonds like C−N and C−O rather than C−C bonds, and they do not involve much of the gold atoms. This is a feature different from what is reported on similar complexes with natural DNA bases.[13b]

Small molecules such as H_20 and HF, when trapped inside spherical clusters such as fullerenes, are known to exhibit contraction in their volumes with blue shifts in stretching frequencies and shortening of bond lengths.[21] This is in contrast to the behavior seen with the Au atoms anchored to the natural bases in DNA as well as x-DNA. Some features in the optimized structures are similar to those seen by Krüger et al.,[15] for example, zigzag structures formed by Au atoms as well as similar Au−Au distances.

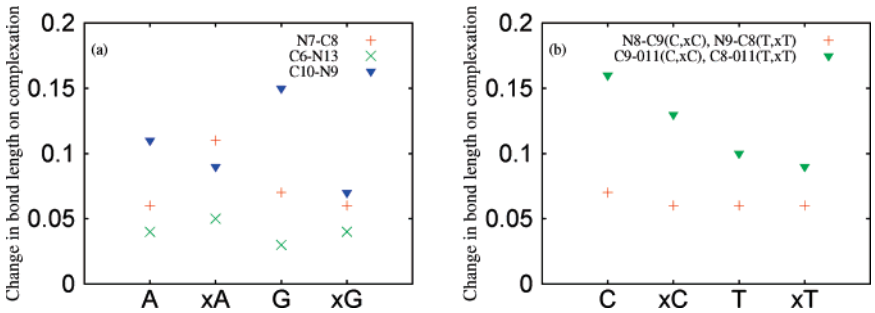

Figure 3. Change in bond length for selected atoms in natural and expanded purines (a) and in natural and expanded pyrimidines (b) on gold complexation.

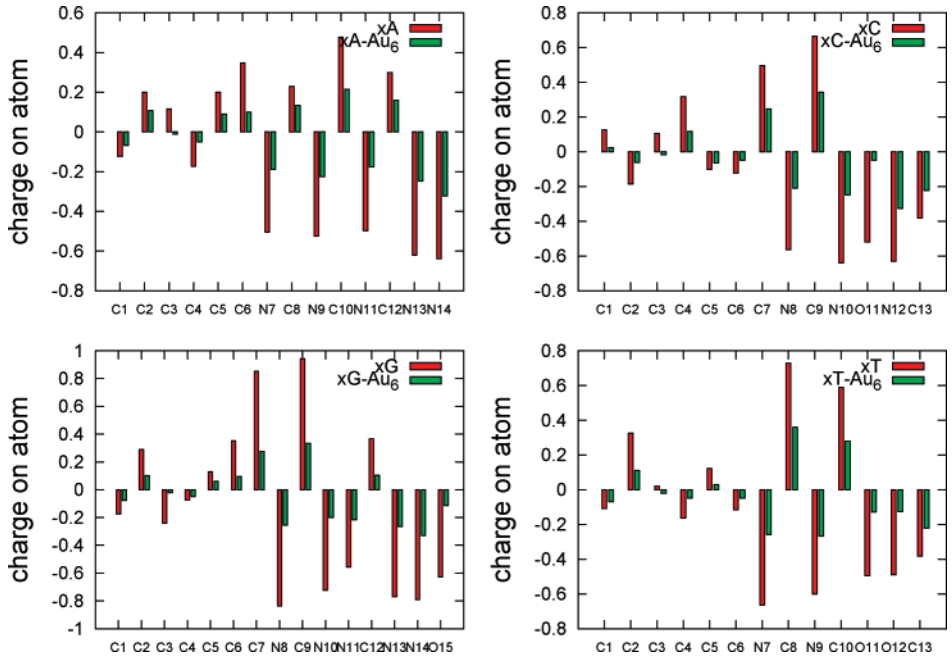

Figure 4. Mulliken charges on the atoms of the x-bases before and after gold complexation: (a) xA, (b) xC, (c) xG, and (d) xT.

The optimized complexes with gold atoms near natural DNA bases, using the same level of theory (see Figure S1) as above, show that the gold atoms form two equilateral triangles of three atoms on each side of the base in all cases, and the gold clusters are completely out of the plane of the bases. This is in contrast with the structures obtained in the case of xA-Au_6 and xC-Au_6 complexes, where the gold atoms are in the plane of the x-base. The presence of the aromatic benzene ring together with the heterocyclic rings (extension in the pyrimidines and in between the purines) provides additional stability due to delocalization of the electron density when the complex is planar. With xC-Au_6 and xG-Au_6, the triangular geometry of gold cluster seen in the case of the natural bases is not retained, and gold clusters acquire irregular structures. Expansion in bond lengths is observed in the case of natural DNA bases on complexing with gold atoms, as observed here in the case of the x-bases. To get a clear picture we plotted some of the changes in bond lengths. The increase in bond lengths for the selected common atoms of purines and x-purines are plotted in Figure 3(a), and the corresponding increase for selected common atoms for pyrimidines and x-pyrimidines are plotted in Figure 3(b). It is found that the C9−N10 bond of xG undergoes much less (nearly half) deviation than the corresponding bond in natural guanine, and the N7−C8 bond of xA undergoes greater expansion than natural adenine. The C9−N10 bond of natural cytosine undergoes much greater expansion on complex formation than the corresponding bond in the expanded bases xC and xT and natural thymine. However, the length of the bond between the N atom linked to a gold atom covalently and the adjacent carbon atom undergoes similar deviation in all cases.

Electronic Charge Distributions. A detailed analysis of the charge distributions in the uncomplexed and gold complexed x-bases was carried out using the Mulliken population analysis scheme.

In the case of xA-Au_6, we find that a substantial overall amount of charge (0.9 e, where e is the electronic charge) is transferred from x-adenine to the gold clusters. The carbon atoms of the x-adenine lose a lesser amount of electron density, in fact some of them show a gain, whereas the nitrogen atoms lose a greater charge (Table S3). This is due to the vicinity of the gold atoms to the N atoms. The $Au_{3(22-24)}$ cluster acquires a negative charge amounting to 0.37e units, whereas the other Au_3 cluster acquires 0.54e of charge. Generally, the gold atom bound to an electron rich site is found to withdraw electrons from the site and acquires negative charge. The N11 and N7 atoms bonded to gold atoms lose about 0.32e of charge to the nearest gold atoms, and the N13 and N9 atoms at the beta positions lose more than 0.3e of charge after redistribution of electron populations. These observations indicate the presence of charge-transfer interactions between gold clusters and x-adenine.

In the case of xC, there is an overall charge loss of 0.95e from the base to the gold clusters. The O atom loses charge amounting to half an electronic charge, as compared to the charge carried by it before gold complexation. The N8 bonded to the gold atom and the nitrogen atoms at the beta positions, N10 and N12, lose more than 0.3e charge each. The $Au_{3(23-25)}$ cluster gains 0.29e units of negative charge, whereas the other Au_3 cluster gains 0.66e units of electronic charge. The triangular structure of the former cluster does not permit a large amount of charge to accumulate as this will give rise to a high charge density as opposed to the open chain case of the latter.

In the case of xG, 0.87e of negative charge is transferred from xG to Au cluster. The N atoms 8, 10, 13, 14, and 015 atoms lose nearly half an electronic charge, and the N11 atom loses 0.34 e of charge. Interestingly, in this case, the C7 and C9 atoms in the vicinity of the covalent linkage between N and Au atoms also lose fairly high amounts of positive charge

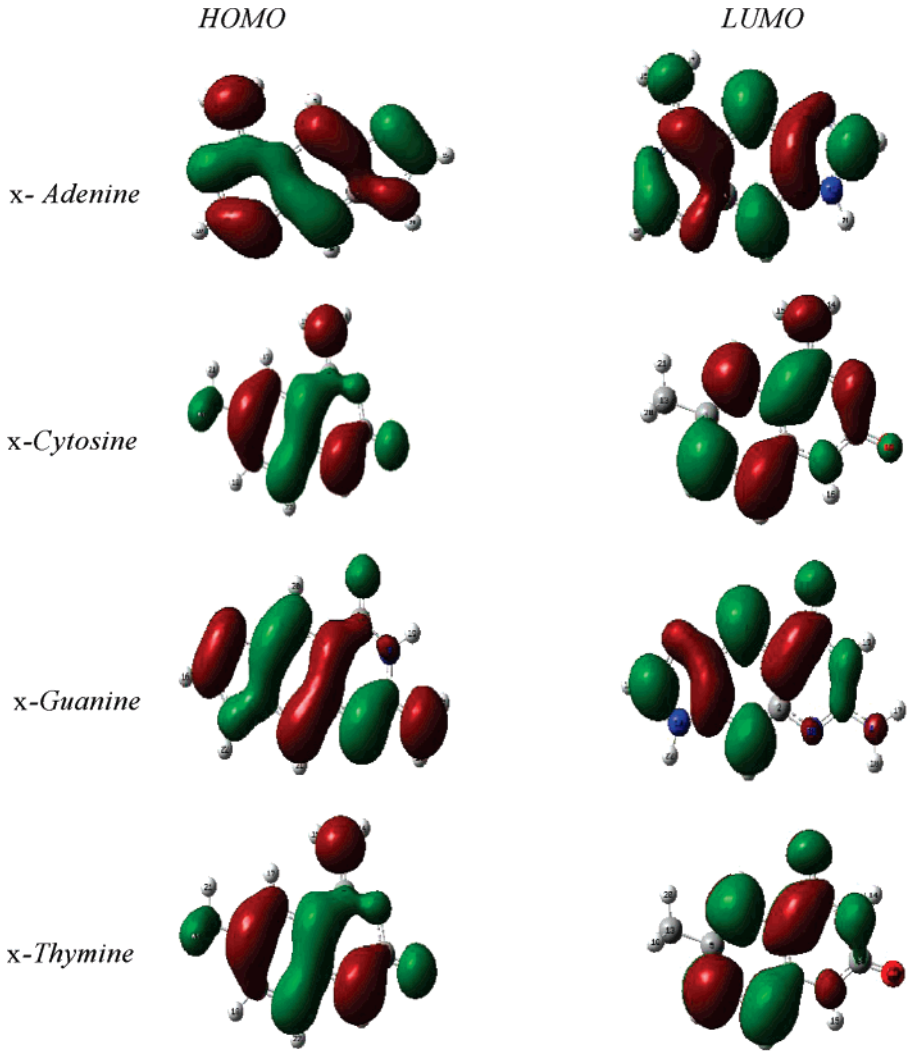

Figure 5. Plots of the highest occupied molecular orbital (HOMO) and the lowest unoccupied molecular orbital (LUMO) for expanded bases x-adenine, x-cytosine, x-guanine, and x-thymine.

(gaining electron density), namely 0.57e and 0.61e respectively, unlike the carbon atoms in the case of xA and xC.

The case of xT is distinct because here the binding with the gold atoms does not involve the N atoms; it is entirely with the O atoms. The N7 and N9 atoms lose 0.41e and 0.37e and C8 and C10 lose 0.33e and 0.31e positive charge (gaining electron density) on gold complexation. Both O11 and O12 atoms lose relatively less, namely 0.36 e charge on gold complexation, nearly the same as the analogous N atoms bound to a gold atoms in the case of xA and xC. A total of 0.82 e is transferred from xT to the gold cluster.

These observations suggest a massive redistribution of electronic charge when the x-bases come in contact with gold atoms. The charge distributions suggest that the gold clusters are stabilized around the x-bases due to electrostatic attractions between the gold atoms and x-base atoms. The Mulliken charges for some selected common atoms of purines have been plotted in Figure 3(c), whereas the corresponding values for selected common atoms for pyrimidines have been shown in Figure 3(d). It is seen that the N14 atom of xG loses a greater amount of charge on gold complexation than the corresponding atom in xA. On the other hand, the decrease in Mulliken charge on the O11 atom in the case of xC is greater than in the case of xT.

In all the expanded bases, the polarization in the six-member benzenoid ring is reduced significantly; this is consistent with the greater aromatic character found with NICS calculations discussed later.

Molecular Orbital Plots. Plots of the highest occupied molecular orbital (HOMO) and the lowest unoccupied molecular orbital (LUMO) of the x-bases are given in Figure 5. It can be seen that there exists a strong intermixing between the atomic orbitals of the x-bases in the frontier molecular orbitals.

Plots of HOMO, HOMO-1, and LUMO for the gold complexed geometry are shown in Figure 5. The frontier orbitals reflect the reactive properties and sensitivity toward neighboring entities in larger assemblies. In contrast to findings on natural DNA bases,[13b] we find that the HOMO and LUMO of xA-Au_6 does not significantly involve the atomic orbitals of the Au atoms. The interaction of Au orbitals with those of the base is maximal in the HOMO of xG-Au_6, and it is found to be antibonding in nature, while for xT-Au_6 and xC-Au_6 it is marginal. The situation changes considerably on excitation, and a greater mixing of Au atomic

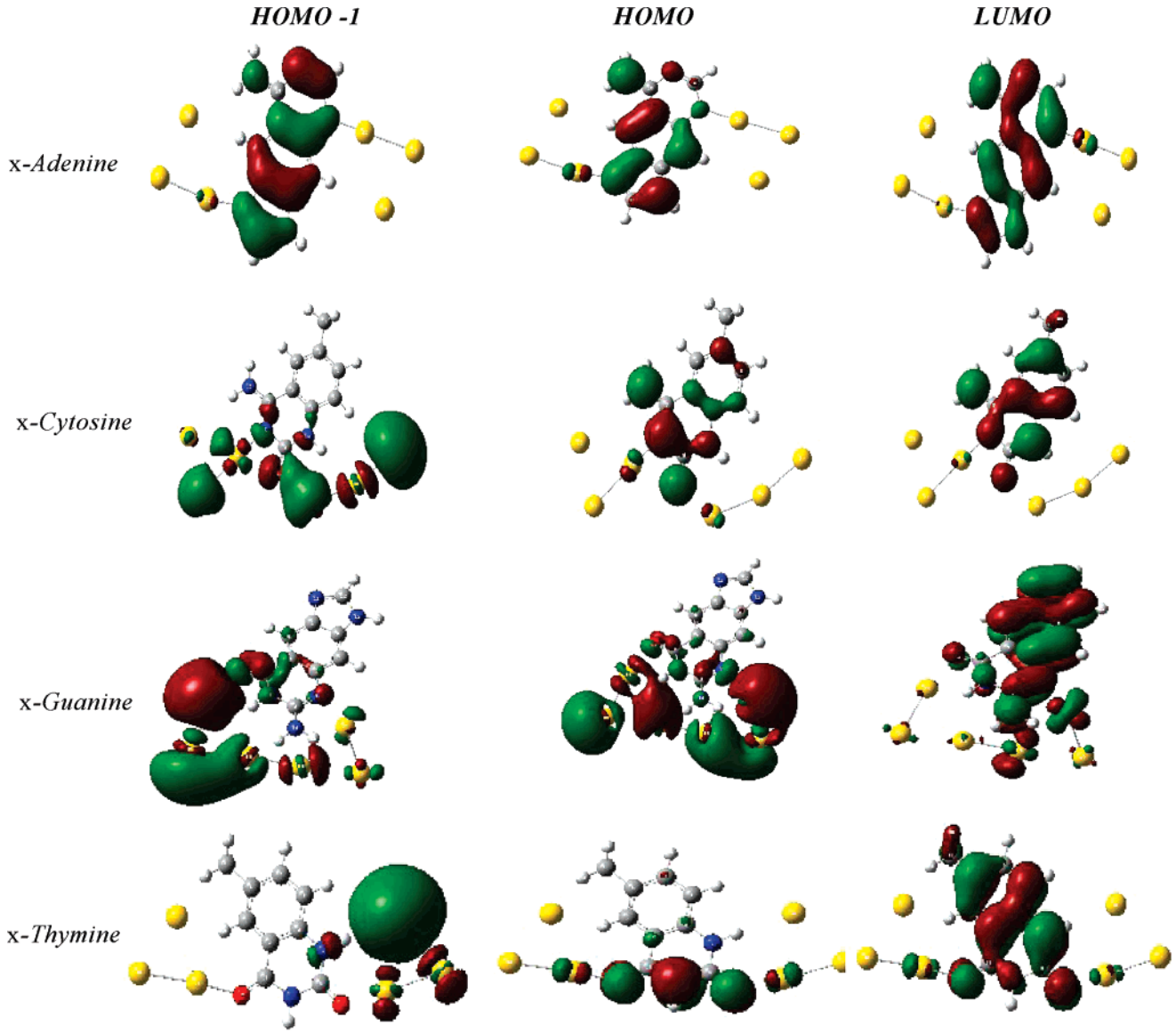

Figure 6. Plots of the frontier molecular orbitals HOMO-1, HOMO, and LUMO for the gold complexes of the expanded bases: x-adenine-Au_6, x-guanine-Au_6, x-cytosine-Au_6, and x-thymine-Au_6.

orbitals is seen in LUMO and LUMO+1 orbitals of the complex. For the xC-Au_6, the HOMO-1 and LUMO show some interaction between the gold atomic orbitals and those of the base. There is a significant intermixing of the atomic orbitals of gold as well as the x-base orbitals in the case of HOMO-1 and LUMO orbitals of the xG-Au_6 complex, but the HOMO is more localized on the gold atoms in this case. The HOMO and LUMO of xT show substantial bonding between gold atoms and xT atoms, but the HOMO-1 is more localized on the gold cluster. The HOMO−LUMO gap for xA-Au_6, xC-Au_6, xG-Au_6, and xT-Au_6 clusters are 0.27, 1.09, 2.92, and 0.27 eV, respectively, at the B3LYP/LanL2MB level. The HOMO−LUMO gaps for free x-bases are found to be 4.35, 4.62, 4.68, and 5.22 eV for xA, xC, xG, and xT, respectively, at the same level of theory. It may be noted that, as the HOMO−LUMO gap in these complexes is too small, this indicates that even a slight amount of thermal energy input can even excite the electrons to higher levels in these complexes. The smaller HOMO−LUMO gap in these complexes could facilitate band transport and charge migration in gold bound xDNA. This suggests the possible use of gold bound size-expanded DNA structures as nanowires.

Vibrational Analysis. Vibrational analysis has been carried out on the optimized structures of the x-bases, in order to examine the effect of gold complexation on stretching frequencies of certain functional groups present in x-bases (Table 2). It has been found that the stretching frequencies of amino as well as carbonyl groups get red-shifted on complexation of the x-bases with gold atoms. This is expected from the general lengthening of the bond distances observed and discussed earlier. The stretching frequencies of carbonyl groups in xC and xG get red-shifted by 226.08 cm^{-1} and 206.51 cm^{-1}, respectively, and the stretching frequencies of the two carbonyl groups of xT get red-shifted slightly (C8−O11 and C10−O12, respectively, by 174.76 and 184.43 cm^{-1}). Similarly, the stretching frequencies of the NH_2 groups of xA, xC, and xG also get shifted to lower

Table 2. Vibrational Frequencies of Some Selected Bonds in Free Bases and Gold Complexed x-Bases

bond	xA (cm^{-1})	xA-Au_6 (cm^{-1})	difference (cm^{-1})
NH2 antisymmetric stretch	3948.80	3842.63	106.17
NH2 symmetric stretch	3729.26	3599.63	129.63
bond	xC (cm^{-1})	xC-Au_6 (cm^{-1})	difference (cm^{-1})
NH2 antisymmetric stretch	3951.55	3878.48	73.07
NH2 symmetric stretch	3728.02	3629.85	98.17
N10−C16	3729.69	3510.89	218.8
C9−O11	1831.54	1605.46	226.08
bond	xG (cm^{-1})	xG-Au_6 (cm^{-1})	difference (cm^{-1})
NH2 antisymmetric stretch	3954.71	3779.30	175.41
NH2 symmetric stretch	3735.08	3592..99	142.09
N8−H19	3714.46	3611.73	102.73
C7−O11	1836.39	1629.88	206.51
bond	xT (cm^{-1})	xT-Au_6 (cm^{-1})	difference (cm^{-1})
N7−C15	3762.43	3459.37	303.06
C8−O11	1886.73	1711.97	174.76
C10−O12	1822.55	1638.12	184.43

wave numbers. These results provide information about the difference in behavior of the x-bases in the gold complexed and free state.

Aromatic Character of the x-Bases. To quantify the aromatic nature of the rings (at their ring centers) of the x-bases before and after complexation to the Au clusters, the nucleus independent chemical shifts (NICS)[17] are calculated at the centers of five- and six-member rings of the x-bases. NICS is a computational method that calculates the chemical shift of a hypothetical ghost atom positioned inside the ring. It is one of the methods of measurement of relative aromaticity of different rings with respect to the observed ring current. The more the negative value of NICS, the greater will be the aromaticity of the ring. The NICS values of five- and six-member rings are given in Table 3. It can be seen that on complexation with gold atoms, the aromatic character of the six-member carbon rings of the x-base increases, but the aromaticity of the five-member rings in the x-bases decreases in the case of purine x-bases. The aromaticity of the six-member heterocyclic ring increases in the case of xG, but it remains the same in the case of xA. On the other hand, the aromaticity of both the six-member carbon rings as well as the six-member heterocyclic rings increases on complexation with gold atoms. These calculations suggest a contribution of electronic effects, to the overall molecular expansion of the x-bases on gold complexation. We point out that the natural purine bases have been reported to become less aromatic, whereas natural pyrimidine bases become more aromatic on complexation with gold atoms.[13b]

Bonding and Interactions. We carried out NBO analysis of the xB-Au_6 complexes and recorded the data on interactions between gold clusters and x-bases. We look at the second-order perturbative estimates of the donor−acceptor (bond−antibond) interactions from NBO analysis to investigate the charge-transfer interactions between gold clusters and atoms of the x-bases. Since these interactions lead to donation of occupancy from the localized NBOs of the idealized Lewis structure into the empty non-Lewis orbitals (and thus, to departures from the idealized Lewis structure description), they are referred to as "delocalization" corrections to the zeroth-order natural Lewis structure. For each donor NBO (i) and acceptor NBO (j), the stabilization energy $E(2)$ associated with delocalization ("2e-stabilization") $i \rightarrow j$ is estimated as[19]

$$E(2) = \Delta E_{i,j} = \frac{-q_i(F(i,j))^2}{E_j - E_i}$$

where q_i is the donor orbital occupancy; E_i and E_j are diagonal elements (orbital energies); and $F(i,j)$ is the off-diagonal NBO Fock matrix element.

The values of $E(2)$, $F(i,j)$, and $E_j - E_i$ for the predominant charge-transfer interactions between the x-bases and gold atoms are given in Table 4 with more details in Table S4 in the Supporting Information. We look at the charge-transfer interactions between the gold clusters and the atoms of the x-base in order to explore the possibility of hydrogen bonding and to understand the nature of interactions between them.

We observe that a significant charge transfer takes place from the lone pair of N7 in xA to antibonding orbitals of Au22−Au23. In addition, charge transfer from the lone pair of electrons in N11 to the antibonding orbital of Au25−Au27 is also seen. The hydrogen bonding interactions between C4−H1...Au26 as well as between N14−H17...Au26 also contribute to the stability of these clusters. In the case of xC, charge-transfer interactions from the lone pair on O11 to the antibonding orbital of Au23−Au24 and Au25−Au28 are the most significant. The hydrogen bonding interactions N10−H16...Au26 and N10−H16...Au28 are also seen in this case. In the case of xG, the charge-transfer interactions from the lone pair of O15 to the antibonding orbitals of Au23−Au24 is the most prominent. The charge transfers from the bonding orbital localized on C9−N10 to the antibonding orbitals of Au26−Au27 and from the lone pair of N10 to the antibonding orbital of Au26−Au27 are also significant. The hydrogen-bonding N8−H19...Au23 is also among the major interactions present in the xG-Au6 complex. In the case of xT, the major charge transfer takes place from the lone pair of O12 to the antibonding orbital of Au23−Au24 and from the lone pair of O11 to the antibonding orbital of Au25−Au27. Hydrogen bonding interactions N7−H15...Au26 and C4−H6...Au23 are also seen.

These observations suggest that the binding between x-DNA nucleobases and gold atom clusters is mostly due to the direct covalent bonds of Au−N or Au−O type. A variety of effects such as charge transfer as well as electrostatic effects and unconventional interactions such as N−H···Au hydrogen-bonding contribute to the stability of the complexes.

Table 3. NICS Calculations for x-Bases before and after Complexation with Gold Atoms

	xA		xG		xC		xT	
ring type	before	after	before	after	before	after	before	after
5-member	−9.57	−9.44	−9.78	−8.96				
6-member carbon ring	−9.68	−11.13	−9.27	−12.40	−7.81	−9.31	−8.03	−8.72
6-member heterocyclic	−4.22	−4.22	−1.08	−2.10	0.08	−3.33	−0.10	−3.87

Table 4. Selected Data from NBO Analysis for xA in Gold Complexed Geometry

	interaction (BD: bonding; LP: lone pair)		second-order interaction (kcal/mol)		
			$E^{(2)}$	$E_j - E_i$	F_{ij}
xA-Au_6	LP N 7	BD* Au22−Au23	82.88	0.40	0.165
	LP N11	BD* Au25−Au27	79.05	0.42	0.163
	LP N8	BD*Au23−Au24	69.83	0.39	0.148
xC-Au_6	LP O11	BD*Au23−Au24	11.05	0.12	0.033
	LP O11	BD*Au25−Au28	68.45	0.06	0.064
	LP O15	BD* Au23−Au24	12.61	0.60	0.083
	LP O15	BD* Au23−Au24	60.76	0.23	0.107
xG-Au_6	BD C9−N10	BD* Au26−Au27	17.87	0.24	0.061
	LP N10	BD* Au26−Au27	57.92	0.37	0.132
	LP O12	BD*Au23−Au24	16.38	0.56	0.091
xT-Au_6	LP O12	BD*Au23−Au24	65.81	0.27	0.120
	LP O11	BD*Au25−Au27	13.93	0.60	0.087
	LP O11	BD*Au25−Au27	73.47	0.25	0.122

5. Conclusion

In this paper, we have presented the first ab initio study of the binding with gold clusters, of size-expanded bases xA, xC, xG, and xT, where an additional benzenoid ring is inserted as compared to the bases of natural DNA. These bases have already been used experimentally to synthesize a new type of DNA called xDNA. There are some similarities and several clear differences in bonding in these complexes compared to bonding in complexes of gold atoms with the natural DNA bases. We find that the bond lengths of the x-bases expand on gold complexation. There is a significant intermixing of orbitals of gold and the x-base in these complexes in lower lying molecular orbitals. However, in clear contrast to the complexes with natural DNA bases, the frontier orbitals do not show a significant mixing of orbitals of the atoms on the expanded bases and those of Au atoms. It seems that most of the mixing must be occurring at lower energy levels, or excitation may result in greater mixing. The HOMO−LUMO gap of gold complexed x-bases is smaller than the free x-bases, thus opening up avenues for exploration of properties like enhanced conductivity in xDNA tagged by gold atoms. There is an appreciable amount of charge transfer from the x-base to gold atoms in all the complexes. The stretching frequencies of the amino and carbonyl groups of the x-bases get red-shifted on gold complexation. The aromatic character of rings in polycyclic x-bases increases on gold complexation. The stability of the complexes is best explained using results from natural bond orbital analysis. It is found that the binding between gold clusters and x-bases has substantial contribution from noncovalent interactions, in addition to the direct covalent bonding between N or O atoms and Au atoms in these complexes. Hydrogen bonding interactions like N−H...Au are likely to play a significant role in the stability of the complexes. We are hopeful that our findings will be of significant relevance to further the understanding of macromolecular assemblies. Further investigations exploring the robustness of these findings with respect to variation of the number of gold atoms in the clusters are desired.

Acknowledgment. H.S. wishes to thank Prof. Biman Bagchi of SSCU, IISc, Bangalore, for his valuable comments as well as his crucial role in getting us involved with nanocluster tagged DNA systems.[22] We thank the CDAC, Pune for computational support and CSIR, New Delhi for JRFs to P.S. and S.S. We also thank the referees for their wise and useful suggestions.

Supporting Information Available: Cartesian coordinates and NBO analysis data of gold complexed x-bases and comparison of the bond lengths and Mulliken charges of all the atoms of free and gold complexed x-bases (Tables S2 and S3). This material is available free of charge via the Internet at http://pubs.acs.org.

References

(1) (a) Ratner, M.; Ratner, D. *Nanotechnology: A Gentle Introduction to the Next Big Idea*; Prentice Hall: Upper Saddle River, NJ, 2002. (b) Tour, J. M. *Molecular Electronics: Commercial Insights, Chemistry, Devices, Architecture and Programming*; World Scientific: River Edge, NJ, 2003.

(2) (a) Egholm, M.; Buchart, O.; Christensen, L.; Behrens, C.; Freier, S. M.; Driver, D. A.; Berg, R. H.; Kim, S. K.; Norden, B.; Nielsen, P. E. *Nature* **1993**, *365*, 566. (b) Nielsen, P. E.; Egholm, M.; Buchart, O. *Bioconjugate Chem.* **1994**, *5*, 3.

(3) (a) Petersen, M.; Wengel, J. *Trends Biotechnol*. **2003**, *21*, 74. (b)Schoning, K.; Scholz, P.; Guntha, S.; Wu, X.; Krishnamurthy, R.; Eschenmoser, A. *Science* **2000**, *290*, 134. (c) Eschenmoser, A. *Science* **1999**, *284*, 2118.

(4) (a) Liu, H.; Gao, J.; Maynard, L.; Saito, D. Y.; Kool, E. T. *J. Am. Chem. Soc.* **2004**, *126*, 1102. (b) Liu, H.; Gao, J.; Lynch, S. R.; Saito, Y. D.; Maynard, L.; Kool, E. T. *Science* **2003**, *302*, 868. (c) Liu, H.; Gao, J.; Lynch, S. R.; Kool, E. T. *J. Am. Chem. Soc.* **2004**, *126*, 6900. (d) Gao, J.; Liu, H.; Kool, E. T. *J. Am. Chem. Soc*. **2004**, *126*, 11826. (e) Liu, H.; Gao, J.; Kool, E. T. *J. Am. Chem. Soc.* **2005**, *127*, 1396. (f) Liu, H.; Gao, J.; Kool, E. T. *J. Org. Chem.* **2005**, *70*, 639. (g) Lee, A. H. F.; Kool, E. T. *J. Am. Chem. Soc.* **2005**, *127*, 3332. (h) Gao, J.; Liu, H.; Kool, E. T. *Angew. Chem., Int. Ed*. **2005**, *44*, 3118.

(5) Liu, H.; He, K.; Kool, E. T. *Angew. Chem., Int. Ed*. **2004**, *43*, 5834. (b) Lee, A. H. F.; Kool, E. T. *J. Org. Chem.* **2005**, *70*, 132.

(6) Lynch, S. R.; Liu, H.; Gao, J.; Kool, E. T. *J. Am. Chem. Soc.* **2006**, *128*, 14704.

(7) Braun, E.; Eishen, Y.; Sivan, U.; Ben-Yoseph, G. *Nature* **1998**, *391*, 775.

(8) Richter, J.; Mertig, M.; Pompe, W.; Monch, I.; Schackert, H. K. *Appl. Phys. Lett*. **2001**, *78*, 536.

(9) (a) Adessi, C. H.; Walch, S.; Anantram, M. P. *Phys. Rev. B* **2003**, *67*, 081405. (b) Health, J. R.; Ratner, M. A. *Phys. Today* **2003**, 43. (c) Long, Yi-T.; Li, C.-Z.; Kraatz, H.-B.; Lee, J. S. *Biophys. J*. **2003**, *84*, 3218. (d) Moreno-Herrero, F.; Herrero, P.; Moreno, F.; Colchero, J.; Gomez-Navarro, C.; Gomez-Herrero, J.; Baro, A. M. *Nanotechnology* **2003**, *14*, 128.

(10) (a) Hou, S.; Zhang, J.; Li, R.; Ning, J.; Han, R.; Shen, Z.; Zhao, X.; Xue, Z.; Wu, Q. *Nanotechnology* **2005**, *16*, 239. (b) Reed, M. A.; Zhou, C.; Miller, C. J.; Burgin, T. P.; Tour, J. M. *Science* **1997**, *278*, 252. (c) DiVenta, M.; Pantelides, S. T.; Lang, N. D. *Phys. Rev. Lett.* **2000**, *84*, 979. (d) Derosa, P. A.; Seminario, J. M. *J. Phys. Chem. B* **2001**, *105*, 471. (e) Xue, Y.; Ratner, M. A. *Phys. Rev. B* **2003**, *68*, 115407. (f) Kerman, K.; Morita, Y.; Takamura, Y.; Ozsoz, M.; Tamiya, E. *Anal. Chim. Acta* **2004**, *510*, 169. (g) Jin, R.; Wu, G.; Li, Z.; Mirkin, C. A.; Schatz, G. C. *J. Am. Chem Soc.* **2003**, *125*, 1643. (h) Garzon, I. L.; Artacho, E.; Beltran, M. R.; Garcia A.; Junquera, J.; Michaelian, K.; Ordejon, P., Rovira, C.; Portal, D. S.; Soler, J. M. *Nanotechnology* **2001**, *12*, 126. (i) Shafai, G. S.; Shetty, S.; Krishnamurty, S.; Shah, V.; Kanhere, D. G. *J. Chem. Phys.* **2007**, *126*, 014704. (j) West, J. L.; Halas, N. J. *Annu. Rev. Biomed. Eng.* **2003**, *5*, 285.

(11) Cabrera-Fuentes, M.; Sumpter, B. G.; Wells, J. C. *J. Phys. Chem. B* **2005**, *109*, 21135.

(12) (a) Demers, L. M.; Östblom, M.; Zhang, H.; Jang, N. H.; Liedberg, B.; Mirkin, C. A. *J. Am. Chem. Soc.* **2002**, *124*, 11248. (b) Storhoff, J. J.; Elghanian, R.; Mirkin, C. A.; Letsinger, R. L. *Langmuir* **2002**, *18*, 6666. (c) Kimura-Suda, H.; Petrovykh, D. Y.; Tarlov, M. J.; Whitman, L. J. *J. Am. Chem. Soc.* **2003**, *125*, 9014. (d) Petrovykh, D. Y.; Kimura-Suda, H.; Whitman, L. J.; Tarlov, M. J. *J. Am. Chem. Soc.* **2003**, *125*, 5219. (e) Chen, Q.; Frankel, D. J.; Richardson, N. V. *Langmuir* **2002**, *18*, 3219. (f) Giese, B.; McNaughton, D. *J. Phys. Chem. B* **2002**, *125*, 1112. (g) Rapino, S.; Zerbetto, F. *Langmuir* **2005**, *21*, 2512. (h) Otero, R.; Schöck, M.; Molina, L. M.; Lægsgaard, E.; Stensgaard, I.; Hammer, B.; Besenbacher, F. A*ngew. Chem., Int. Ed.* **2005**, *44*, 2270. (i) Östblom, M.; Liedberg, B.; Demers, L. M.; Mirkin, C. A. *J. Phys. Chem. B* **2005**, *109*, 15150. (j) Yonezawa, T.; Onoue, S.-Y.; Kimizuka, N. *Chem. Lett.* **2002**,1172.

(13) (a) Kumar, A.; Mishra, P. C.; Suhai, S. *J. Phys. Chem. A* **2006**, *110*, 7719. (b) Mohan, P. J.; Datta, A.; Mallajosyula, S. S.; Pati, S. K. *J. Phys. Chem. B* **2006**, *110*, 18661.

(14) Kryachko, E. S.; Remacle, F. *J. Phys. Chem. B* **2005**, *109*, 22746.

(15) Krüger, D.; Fuchs, H.; Rousseau, R.; Marx, D.; Parrinello, M. *Phys. Rev. Lett.* **2002**, *89*, 186402.

(16) (a) Becke, A. D. *J. Chem. Phys.* **1993**, *98*, 5648. (b) Lee, C.; Yang, W.; Parr, R. G. *Phys. Rev. B* **1988**, *37*, 785. (c) Frisch, M. J.; Trucks, G. W.; Schlegel, H. B.; Scuseria, G. E.; Robb, M. A.; Cheeseman, J. R.; Zakrzewski, J. A.; Montgomery, J. A., Jr.; Stratmann, R. E.; Burant, J. C.; Dapprich, S.; Millam, J. M.; Daniels, A. D.; Kudin, K. N.; Strain, M. C.; Farkas, O.; Tomasi, J.; Barone, V.; Cossi, M.; Cammi, R.; Mennucci, B.; Pomelli, C.; Adamo, C.; Clifford, S.; Ochterski, J.; Petersson, G. A.; Ayala, P. Y.; Cui, Q.; Morokuma, K.; Malick, D. K.; Rabuck, A. D.; Raghavachari, K.; Foresman, J. B.; Cioslowki, J.; Ortiz, J. V.; Stefanov, B. B.; Liu, G.; Liashenko, A.; Piskorz, P.; Komaromi, I.; Gomperts, R.; Martin, R. L.; Fox, D. J.; Keith, T.; Al-Laham, M. A.; Peng, C. Y.; Nanayakkara, A.; Gonzalez, C.; Challacombe, M.; Gill, P. M. W.; Johnson, B. G.; Chen, W.; Wong, M. W.; Andres, J. L.; Head-Gordon, M.; Replogle, E. S.; Pople, J. A. *Gaussian03, Revision B.05*; Gaussian, Inc.: Pittsburgh, PA, 2003.

(17) Schleyer, P. v. R.; Maerker, C.; Dransfeld, A.; Jiao, H.; Hommes, N. J. R. v. E. *J. Am. Chem Soc.* **1996**, *118*, 637.

(18) (a) Gomes, J. A. N. F.; Mallion, R. B. *Chem. Rev.* **2001**, *101*, 1349. (b) Lazzeretti, P. *Prog. Nucl. Magn. Reson. Spectrosc*. **2000**, *36*, 1. (c) Krygowski, T. M.; Cyranski, M. K. *Phys. Chem. Chem. Phys*. **2004**, *6*, 249. (d) Chen, Z.; Wannere, C. S.; Corminboeuf, C.; Puchta, R.; Schleyer, P. v. R. *Chem. Rev.* **2005**, *105*, 3842.

(19) (a) Reed, A. E.; Weinstock R. B.; Weinhold, F. *J. Chem. Phys.* **1985**, *83*, 735. (b) Reed, A. E.; Curtsiss L. A.; Weinhold, F. *Chem. Rev.* **1988**, *88*, 899.

(20) Barranco, E. M.; Crespo, O.; Gimeno, M. C.; Jones, P. G.; Laguna, *Eur. J. Inorg. Chem.* **2004**, *2004*, 4820.

(21) (a) Shameena, O.; Ramachandran, C. N.; Satyamurthy, N. *J. Phys. Chem. A* **2006**, *110*, 2. (b) Sen, K. D. *J. Chem. Phys*. **2005**, *122*, 194324.

(22) (a) Singh, H.; Bagchi, B. *Curr. Sci*. **2005**, *89*, 1710. (b) Saini, S.; Singh, H.; Bagchi, B. *J. Chem. Sci.* **2006**, *118*, 23.

CT700145E